THE DEVELOPMENT OF TRANSONIC AIRFOILS FOR HELICOPTERS

J. W. Sloof
Senior Research Engineer
Netherlands National Aerospace Laboratory (NLR)
Amsterdam, Netherlands

Prof. Dr.-Ing. F. X. Wortmann
Institut fur Aerodynamik u. Gasdynamik
der Universitat Stuttgart
Stuttgart, West Germany

J. M. Duhon
Aerodynamics Group Engineer
Bell Helicopter Company
Fort Worth, Texas

PRESENTED AT THE 31st ANNUAL NATIONAL FORUM
OF THE
AMERICAN HELICOPTER SOCIETY
WASHINGTON D.C.
MAY 1975

PREPRINT NO. 901

THE DEVELOPMENT OF TRANSONIC AIRFOILS FOR HELICOPTERS

J. W. Sloof
Senior Research Engineer
Netherlands National Aerospace Laboratory (NLR)
Amsterdam, Netherlands

Prof. Dr.-Ing. F. X. Wortmann
Institut fur Aerodynamik u. Gasdynamik
der Universitat Stuttgart
Stuttgart, West Germany

J. M. Duhon
Aerodynamics Group Engineer
Bell Helicopter Company
Fort Worth, Texas

Abstract

This paper presents two approaches to the design of helicopter main rotor blade airfoils which attempt to satisfy specific design criteria in the transonic regime. The successful design of such airfoils results in significant performance improvements. Examples of power required savings are discussed. One of the two design approaches is offered by Dr. F. X. Wortmann which is a simplified three-step method to achieving shockless flow for the low-lift, high Mach number and the high-lift, moderate Mach number conditions. The second methods, developed at the Netherlands National Aerospace Laboratory (NLR) aims at the same objectives by use of a transonic hodograph method. Airfoils designed by the two methods are described and their qualities are discussed. Performance of a helicopter using such airfoils is analytically determined and compared with more conventional designs.

Notation

$C(x)$	total angular deflection of compression waves between upstream sonic point and x.
c	local compression wave angle airfoil chord
c_ℓ	lift coefficient
c_{m_o}	section pitching moment coefficient about aerodynamic center with subsonic flow on the airfoil at small lift coefficients
c_p	pressure coefficient
c_p^*	pressure coefficient for local M = 1.0
d	airfoil section drag
$E(x)$	total angular deflection of expansion waves between upstream sonic point and x
e	local expansion wave angle
ℓ	airfoil section lift
M	Mach number
R	rotor radius, ft.
R'	radius of curvature
SHP	engine shaft horsepower
x	chord station
x_s	point on airfoil where local velocity is equal to the speed of sound
α	angle of attack
Γ	circulation
ε_o	thickness ratio parameter
λ_1, λ_2	control parameters for use in transonic hodograph theory.
ϕ	airfoil surface slope, deg.
Ω	rotor angular velocity, rad/sec
ω	Prandtl-Meyer angle, deg.

SUBSCRIPTS

∞	free-stream
max	maximum value
min	minimum value
te	airfoil trailing edge

Presented at the 31st Annual National Forum of the American Helicopter Society, May 1975.

Introduction

The technique of designing helicopter airfoils to a particular set of requirements is quite new and much remains to be learned. However, the first steps have been taken and these show considerable promise. One must keep constantly in mind that the airfoil for a helicopter main rotor blade has a wide range of operating conditions within the lift coefficient-Mach number plane. In this plane, there are three primary areas of interest illustrated in Figure 1. These are the maneuver region, the hover design region and the high-speed advancing-blade region. Table 1 presents anticipated values for an airfoil designed specifically for one of the areas shown in Figure 1. Also, in this table are goals for an airfoil designed to be suitable for all three of these key areas.

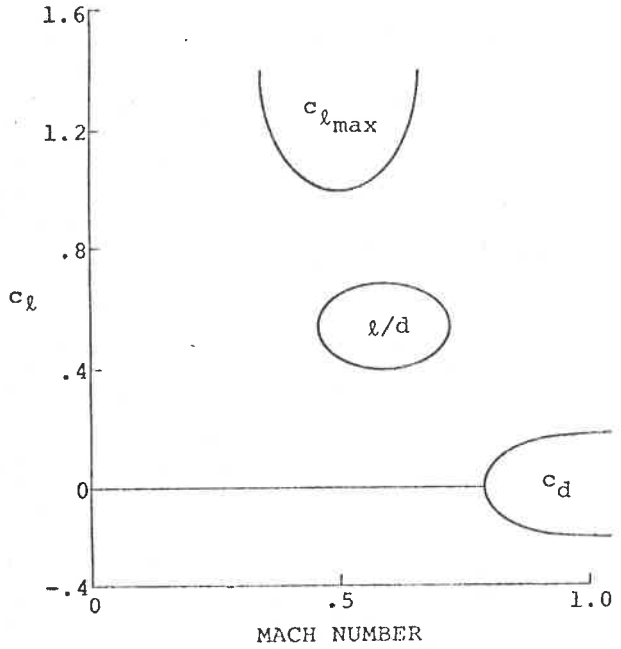

Figure 1. Design regions for a main rotor airfoil.

The first step at Bell Helicopter Company in conjunction with Dr. Wortmann was to design a main rotor airfoil which stressed the hover and maneuver areas. This was reported in Reference 1. The resulting airfoil, the FX69-H-098 (The FX69-H-098 and the FX71-H-090 will be referred to as the FX-098 and FX-090, respectively, in the remainder of this paper.), was a considerable advance over existing main rotor sections and was applied to a research rotor which ultimately was used on the Model 309 KingCobra attack helicopter and the Model 214 utility transport. These applications proved the hover and maneuver advances that were anticipated.

The next step in the airfoil design process was an attempt to increase the drag rise Mach number at low angles of attack without deterioration of the desired hover and maneuver characteristics. This effort was made in 1972 in a NASA-Langley contracted program which involved a joint effort between National Aerospace Laboratory of the Netherlands (NLR) and Bell Helicopter Company. This program led to two airfoil designs - one with unrestricted pitching moments and one with limited pitching moments. Reference 2 summarizes this effort. About the same time in an independent effort, Wortmann, as a consultant to Bell Helicopter, designed airfoils which were also aimed at the same goal - one of which is designated the FX-090.

The NLR and Wortmann design approaches were considerably different and yet resulted in airfoils with quite similar aerodynamic characteristics. This paper covers these two design methods, wind tunnel test results and application criteria for this type of airfoil.

Before proceeding, it must be emphasized that considerably more effort must be made in developing the design procedures and in iterating between test results and analysis to achieve the best designs. To date, this iteration has not been done and the design method limitations reflect

Table 1. Helicopter Airfoil Design Goals.

Flight Condition	Specific	Quantity	Design Goals for Practical Airfoil	Probable Upper Limits for Separate Optimization
Hover	$M_\infty = 0.6$, $c_\ell = 0.65$	c_ℓ/c_d	100	≈ 220
		c_m	$<\|0.02\|$	?
Maneuver	$M_\infty \approx 0.5$	$c_{\ell_{max}}$	>1.35	≈ 2.1
High Speed	$c_\ell \approx 0$, $c_d = 0.013$	M_∞	>0.85	≈ 0.93

this fact. Only when this process has been followed, will one be able to design transonic airfoils for rotors with a minimum of compromise in the hover and maneuver characteristics of the rotor.

Rotor Airfoil Design by F. X. Wortmann

Introduction

It is well known that the blade profiles of a helicopter rotor have to work in a most complicated flow environment (References 1, 3, and 4). At this time, it is impossible to take into account the unsteady and three-dimensional nature of the flow field as it affects airfoil design. Even if the flow is simplified significantly by assuming two-dimensional, steady-state conditions, there remains the basic difficulty of designing a section that has to meet not one, but at least two, widely different design requirements. These are the high speed/zero lift condition on the advancing side and the maneuver lift condition at medium Mach numbers on the retreating side of the rotor disc.

For both sets of conditions, local supersonic fields are unavoidable and Figure 2 typifies the extent of these regions along the surface (Reference 5). Note that these conditions are those that may be critical relative to strong shock-boundary layer interaction. Note also that on the upper surface behind the leading edge there exists an overlap of the supersonic fields, which occurs on the same part of the airfoil for both the high speed/low lift conditions and the extreme high lift condition. It is not yet clear if, and to what extent, a solution could be found which would be compatible with the requirement of shockless flow for both conditions.

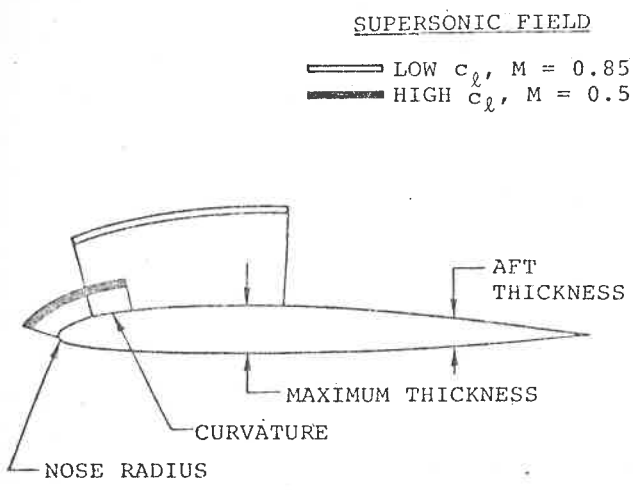

Figure 2. Typical design characteristics.

Despite these seemingly pessimistic circumstances there is some hope of finding solutions for the supersonic flow fields which would avoid the formation of strong shocks. For such cases the powerful methods used to calculate transonic flows, which are available today, are most promising. A survey of these methods is given in Reference 4. It is also obvious that any design procedure must have a simple and fast method to produce, analyze and modify a set of airfoils in order to accelerate the selection process and to approach a final solution. It is the purpose of this part of the paper to describe and supply such a method which largely depends on ideas developed by Pearcey (Reference 6).

Methods and Concepts

The methods and concepts may be divided into three basic steps. The first is to develop the ability to generate, from a chosen velocity distribution, an airfoil shape which nearly realizes the desired velocity in incompressible flow. The singularity method developed by Truckenbrodt (Reference 7) and Riegels (Reference 8) is preferred. It is felt that the lack of precision for cambered airfoils due to a chordwise distribution of vorticity is more than compensated for by the simplicity and flexibility of these methods. To check the results of these methods, the resultant shape may be analyzed by the Theodorsen method yielding an "exact" solution.

With this shape and the corresponding incompressible velocity distribution, the second step may now be taken; that of converting the flow field into a compressible one by means of a similarity rule as given by Labrujere, Loeve and Sloof (Reference 9). These authors show that the NLR-formula holds approximately even for weak supersonic fields.

Assuming the resulting velocities are reliable they can be applied in the third step which is based upon some suggestions made by Pearcey (Reference 6), Pearcey and Osborne (Reference 10) and Sinnot and Stuart (Reference 11).

The local supersonic field on a convex surface is structured by a sequence of expansion waves e(x) which are reflected at the sonic line as compression waves c(x). The combined effect of both wave groups turns the flow parallel to the surface, i.e. the surface slope ϕ equals the sum of the expansion and compression waves

$$\phi(x) = E(x) + C(x),$$

where $E(x) = \sum_{x_s}^{x} e(x)$ and $C(x) = \sum_{x_s}^{x} c(x)$ are

the angular deflections between the upstream sonic point x_s and a given downstream point x. The difference $\omega(x) = E(x) - C(x)$ yields the Prandtl-Meyer angle or the distribution of the local Mach number.

All these qualities can easily be calculated once the geometry of the airfoil and the compressible velocity distribution are known from the first two steps. Up to this point all three steps need a computer time of the order of one second.

It is an open question what physical meaning these calculations have since the simple similarity rules cannot indicate any divergent velocity development or shock appearance. Only in the special case of a shock-free flow do the results reflect a physically meaningful situation.

According to Pearcey and Osborne (Reference 10) three conditions are necessary for a shockless flow:

(1) The value of $\omega(x)$ has to decrease monotonically to zero at the end of the local supersonic field (starting with a smooth incompressible velocity distribution, which yields also a smooth compressible one; this condition is always satisfied and therefore not significant).

(2) The maximum value of ω should stay below 12 degrees or the local Mach number should not exceed the value of 1.5. Spee (Reference 12) has given the physical interpretation that extraneous disturbances must be able to turn and penetrate through the supersonic field against the flow.

(3) The reflected compression waves should not coalesce inside the supersonic field into a shock. This can be ensured by a monotonically decreasing E(x)- distribution ahead of the crest.

Even if the design process starts with a well educated guess, it cannot be expected that the conditions (2) and (3) will be satisfied. Since the whole reflection pattern inside the supersonic field depends both on the velocity distribution and the geometry of the surface, it is not yet clear how to correct the input values to get an improved output with respect to (2) and (3). Fortunately, changes in the velocity input seem to be the overriding factor and generally the supersonic field can easily be modified to get a shockfree appearance.

When this has been achieved, say for the high speed/low lift case, the airfoil has to be investigated for high angles of attack at $M_\infty = .5$ and modified in the nose region in order to obtain another shockless region. As shown in Figure 2 there is an overlap of the two supersonic fields and it cannot be stated to what extent the requirement of shockless flow in both cases is compatible. At this stage it may be best to illustrate the situation by two examples.

Two Design Examples

The geometry of two airfoils is given in Figure 3. The FX-098 was designed with emphasis on high lift values at a Mach number of .5. The design philosophy is outlined in Reference 1. Figures 4 and 5 show the supersonic fields on the upper side at low and high angles of attack at two different Mach numbers. It can immediately be seen that the upper side in Figure 4 is not well suited to the high speed case. At $M_\infty = .75$ and incidences higher than -1^o, i.e., at positive lift values, the situation becomes increasingly worse. For the high lift case, Figure 5 reveals the possibility of an extended shockless supersonic field at $M_\infty = .5$ between $0 < \frac{x}{c} > .16$ at a relatively high angle of attack (up to ten degrees).

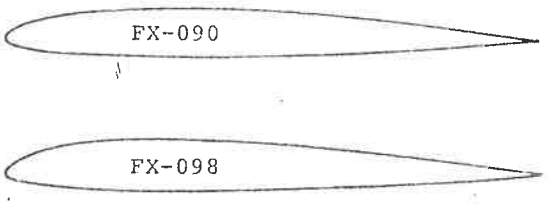

Figure 3. FX-090, FX-098 Comparison

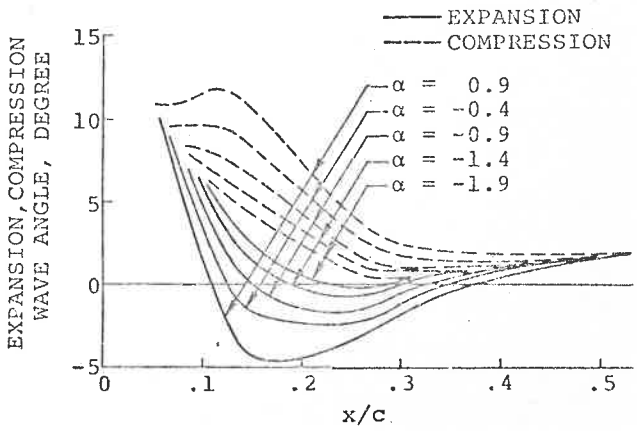

Figure 4. Shape of expansion and compression curves for the high-speed, low-lift case, M = 0.75, FX-098.

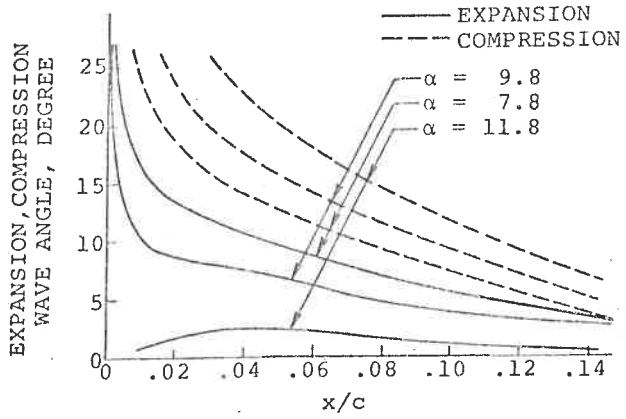

Figure 5. Shape of expansion and compression curves for the high-lift case, M = 0.5, FX-098.

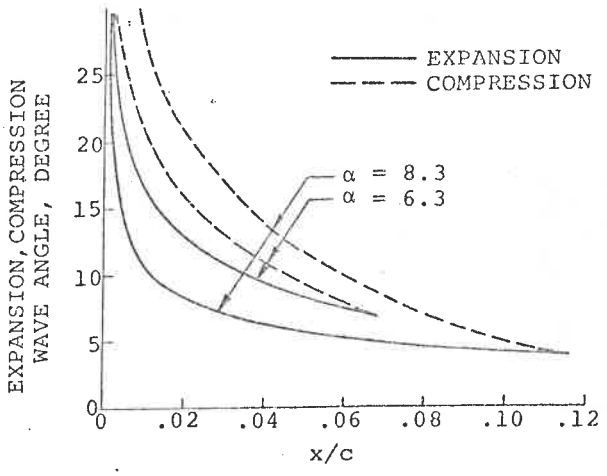

Figure 7. Shape of expansion and compression curves for the high-lift case, M = 0.5, FX-090.

The second airfoil, FX-090, was a first attempt to use the iterative procedure described above in order to combine better high speed characteristics with good $c_{\ell_{max}}$ values. Figures 6 and 7 contain the final results of the selection process. In Figure 6 it can be seen that for a Mach number of .825 and incidences below -.21 degrees there should be good chances for a shock-free flow in the region between $.06 < \frac{x}{c} > 0.35$. For the Mach number .5 and high incidences Figure 7 gives an indication that a shock-free flow may be possible along the chord region between $0 < \frac{x}{c} > .12$ up to incidences of nearly nine degrees.

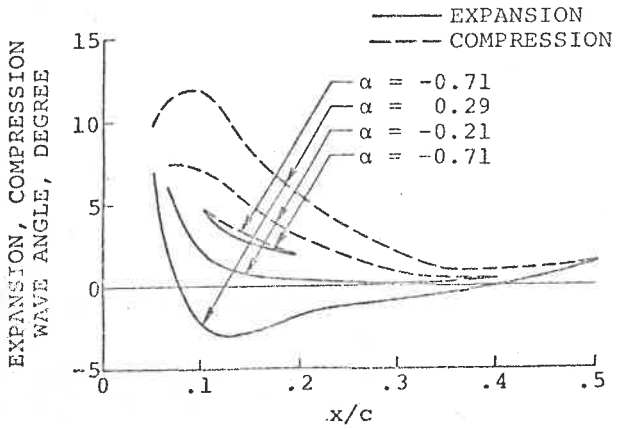

Figure 6. Shape of expansion and compression curves for the high-speed, low-lift case, M = 0.825, FX-090.

Comparing the two designs with each other, it is obvious that the high speed qualities of the FX-090 airfoil have been improved partly at the expense of the high lift capability. On the other side, this example demonstrates at least in the framework of this simple approach, that the same airfoil shape may realize a local supersonic flow field with reduced shock strength as well at high Mach numbers and low incidences as at medium Mach numbers and high angles of attack.

Both airfoils exhibit a typical geometric feature, i.e., the relatively strong curvature near the 10-15% chord station. In reference 13 it has been shown that this characteristic feature is very beneficial for the $c_{\ell_{max}}$ at low and medium Mach numbers. It seems that the existence of this curvature "bump" is also beneficial for the high speed case of the helicopter airfoil.

The effect of the boundary layer has not been considered for two reasons: first, the chosen way to calculate the supersonic field cannot be too accurate and it does not make much sense to introduce, at this stage, the complication of viscous flow; second, the pressure gradients of the two airfoils discussed here are rather soft even at higher values of attack, and the feed-back of the viscous flow will only become serious at the design limits.

The purpose of the paper was to demonstrate that a crude and simple method can be used in the complicated selection process leading to a double purpose airfoil. With-

out doubt the development will be refined by the now available methods to calculate transonic flows and by taking into account the viscous flow which finally should lead to more advanced airfoils for helicopters.

Rotor Airfoil Design by Means of Transonic Hodograph Theory

Introduction

The NLR approach to the rotor airfoil problem differs considerably from Wortmann's technique, in spite of the fact that the objectives are similar. Airfoil design at NLR, for fixed as well as rotary wings, is based on analytical transonic hodograph theory as developed by Nieuwland (Reference 14) and, more recently, as extended by Boerstoel (Reference 15).

In Nieuwland's original hodograph method, the transonic shock-free flow around a so-called quasi-elliptical airfoil (and the airfoil shape itself) is obtained as the result of the transformation of the incompressible potential flow around a lifting ellipse. The airfoil shape and flow field are controlled by four basic and either two or three additional parameters.

The basic parameters are the angle of attack α, circulation Γ, thickness ratio parameter ϵ_o of the ellipse in incompressible flow, and the free stream Mach number M_∞. Profiles defined with these basic parameters generally have to be closed at the trailing edge with additional control parameters. At this point in the design, one has the option of using either two or three parameters to close the airfoil. The choice is governed by whether or not additional control in the nose region is desired. If the three parameter method is chosen then the section may be closed analytically. However, if the two parameter method is used, then the section is not closed completely and has to be closed arbitrarily. This latter method with two control parameters λ_1 and λ_2 was chosen in this study.

In applications of Nieuwland's method it was found that the class of airfoils contained by the theory is generally too limited for practical purposes. It was also found in Reference 16, however, that parts of the basic analytical airfoils can be modified without destroying the low-drag properties of the basic shock-free flow. This last feature was usefully exploited in the rotor airfoil study that is the subject of this paper.

It should be mentioned that since the execution of the present rotor airfoil study in 1972, the analytical hodograph method has been widely extended by Boerstoel. It appears that this new method (Reference 15) does not suffer from the practical limitations originally contained by Nieuwland's method.

The present paper is concerned with the first application of Nieuwland's method to rotor airfoil design. The main purpose of the study (Reference 2) was to generate an airfoil with a zero-lift drag-rise Mach number significantly higher than that of contemporary rotor airfoils. This was to be accomplished with a low aerodynamic pitching moment and, preferably without penalty in hover ℓ/d or retreating blade $c_{\ell_{max}}$.

In the following sections the design process will first be described in detail followed by a discussion of the geometric and aerodynamic characteristics of the resulting airfoil. The flow chart showing in Figure 8 shows the basic logic used for this method.

Outline of Design Procedure

In order to appreciate the following line of thought it is essential to realize that the hodograph method for quasi-elliptical airfoils provides for a given set of input parameters one and only one transonic shock-free shape and corresponding pressure distribution. As mentioned before, one of the input parameters (M_∞) is related to the free stream Mach number and one (Γ) to the circulation around the airfoil. Together they determine a "design point" in the c_ℓ-M_∞ plane. The other parameters can be used to generate a series of shapes with corresponding pressure distributions for the chosen design point in the c_ℓ-M_∞ plane.

In setting the input parameters for the hodograph method, the first question is related to the placement of the design point in the c_ℓ-M_∞ plane. Is this point to be that of the hover, maneuver, high speed condition or at some intermediate condition? With respect to this question some information may be obtained by considering pressure distributions of a typical rotor airfoil (Wortmann FX-098) in the critical regions of the c_ℓ-M_∞ plane. At hover, the transonic effects are strong but the chordwise extent is limited. At high speed there is fully developed transonic flow over most of the upper and lower surfaces. Hence, it may be concluded that the benefits of being able to develop a shape for transonic, shock-free flow could be best exploited at the high speed condition. This applies in particular to the design study reported in Reference 2, where the emphasis was on good high speed characteristics

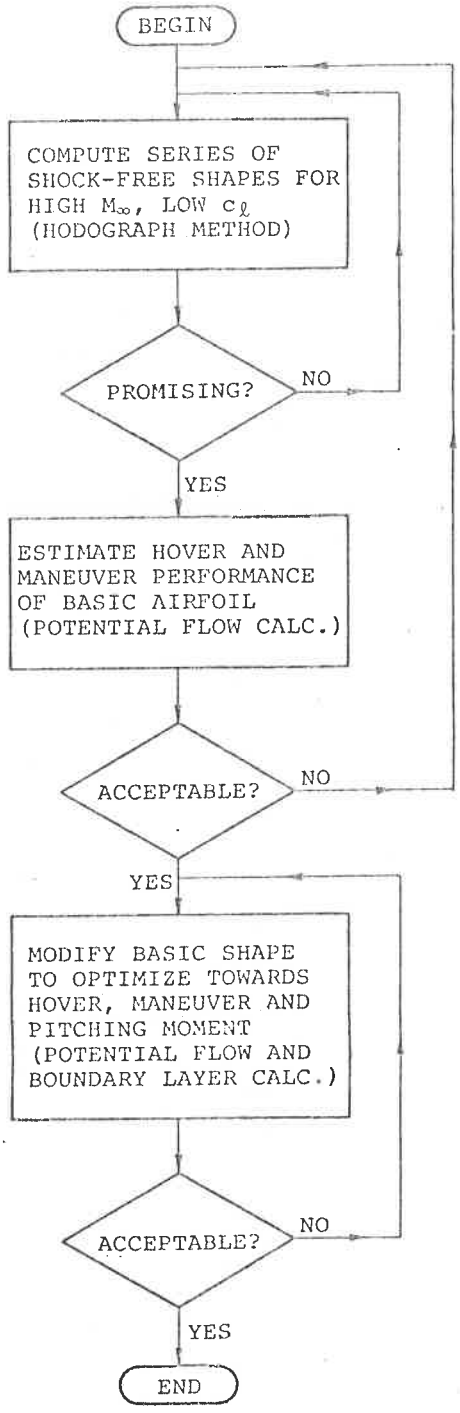

Figure 8. Simplified flow diagram of the NLR airfoil design process.

With the "design point" in the c_ℓ-M_∞ plane fixed, the next step is to calculate by means of the hodograph method a series of shock-free shapes all satisfying the high speed requirement. This step needs systematic variation of the input parameters ϵ_o, α, λ_1, λ_2. By engineering judgment of geometry and pressure distribution the shapes that are most promising are selected for further evaluation. This further evaluation consists of a crude estimate of the hover and maneuver characteristics by means of potential flow calculations. The shape that promises the highest $c_{\ell_{max}}$ at $M_\infty = 0.5$ is then chosen as the basic high speed airfoil. The final step is to modify parts of the basic airfoil with the objective of improving the hover and maneuver performance and keeping the pitching moment within the required limits. This should be done, and by NLR experience can be done, without severe consequences with respect to the drag at the high speed design condition. Such a modification process is one of trial and error in which the effects of a shape modification are analyzed by means of flow computations. Both inviscid, compressible flow and boundary layer calculations are used in this phase.

Results of Hodograph Computations

Experience at NLR has shown that if a drag-rise Mach number of 0.85 is required, the Mach number for the theoretical shock-free design condition can be about 0.025 lower. For this reason, the parameter M_∞ was chosen to be 0.826 in the hodograph calculations. The circulation Γ was kept at a small value. The other parameters were varied such that the geometry and the pressure distribution at the design condition exhibited some of the features of the highly successful FX-098 airfoil.

The best result obtained was an airfoil labelled NLR 7223. Figure 9 presents the shape of this airfoil as well as the sonic lines and pressure distribution at the high speed design condition. Note that the airfoil has a drooped nose and that it is not properly closed at the trailing edge.

Considering the geometry of the nose region in detail, it was found that the upper surface curvature distribution exhibits a remarkable peak at $x/c = 0.096$ ($\sqrt{x/c} \approx 0.31$) as shown in figure 10. This peak is caused by a so-called limit line cusp just inside the airfoil and is of major importance for the shock-free upper surface flow. It may be noted, that a somewhat similar, but less pronounced curvature distribution is exhibited by the FX-098 airfoil. Wortmann, in References 1 and 13, found this to be the key feature for a high $c_{\ell_{max}}$ at moderate Mach numbers.

It is shown in Figure 11 that the chordwise position of the curvature peak is an important parameter with respect to $c_{\ell_{max}}$ at moderate Mach numbers. At a certain Mach number and high angle of attack

HODOGRAPH DESIGN PARAMETERS:

M_∞ = 0.826
ε = 0.695
α = -0.0533 RADIANS
Γ = 0.3
λ_1 = 0.2
λ_2 = -3.5

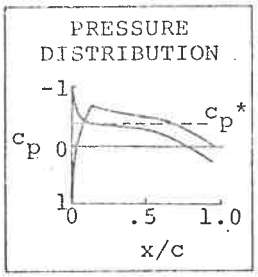

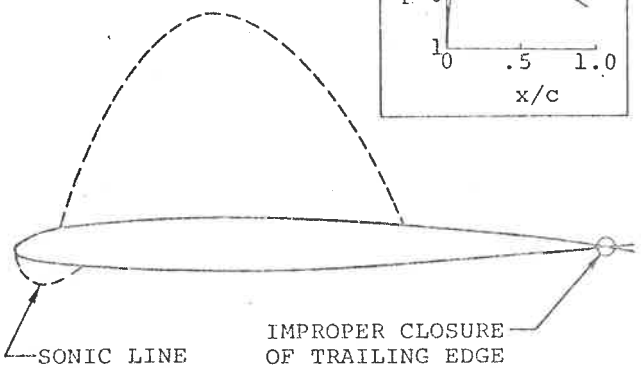

Figure 9. NLR7223 Basic shape at the high-speed design condition.

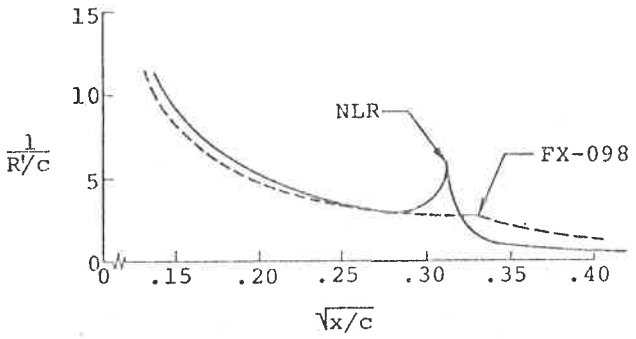

Figure 10. Upper surface curvature distribution.

the downstream end of the supersonic zone near the leading edge coincides with the position of the curvature peak. The expansion effects generated by the curvature peak then tend to decrease the compression effects of the shock. This is an optimum condition with respect to the intensity of the shock. At this optimum condition the width of the supersonic suction region is determined by the distance from the leading edge to the curvature peak, and the larger this distance, the higher the $c_{\ell_{max}}$. In addition to the findings of Wortmann (Reference 1), this is believed to be an important rule for obtaining a high $c_{\ell_{max}}$ in the medium Mach number range.

SHOCK LOCATION
(I) FRONT OF CURV. PEAK
(II) AT CURV. PEAK
(III) AFT OF CURV. PEAK

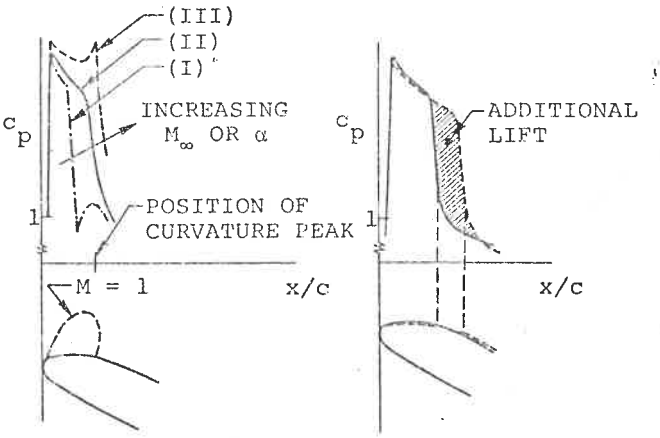

Figure 11. Effect of shock location relative to curvature peak.

It is not clear whether the position of the curvature peak discussed above can be shifted to x/c values beyond 0.10 while maintaining the 0.85 drag-rise Mach number. Within the time available, airfoil 7223 was the best result obtained and was therefore selected as the basic shock-free shape.

Modifications to the Basic Shape

In modifying a basic, shock-free shape the important question is how large a modification can be tolerated if one does not wish to lose the low-drag properties at the high speed design condition. NLR experience in this respect is, that the modification must be limited to the regions that have subsonic flow at the high speed design conditions. For the basic airfoil of Figure 9 this means that the upper surface may be modified aft of approximately 70% chord and the lower surface aft of 20% chord.

The considerations underlying the modifications to the basic shape are listed as follows and also are illustrated in Figure 12.

(1) In order to postpone the appearance of shock waves on the upper surface at moderate Mach numbers and high values of c_ℓ, increase, if possible, the c_ℓ-value for which the flow first becomes critical in the 0.5 to 0.6 Mach number range.

(2) To minimize boundary layer drag at the hover condition, try to realize a laminar, accelerating flow of long extent on the lower surface at $M_\infty = 0.6$, $c_\ell = 0.65$.

(3) To satisfy the pitching moment requirement, reduce, if necessary, the load near the trailing edge.

(4) To reduce the risk of early boundary layer separation at the maneuver and high speed conditions avoid large pressure gradients and apply, if possible, a Stratford (Reference 17) type of pressure recovery.

1. BEGINNING OF SURFACE THAT MAY BE MODIFIED, ①, ②.
2. LIFT ADDED AT ① AND ③ TO POSTPONE SHOCKS AT ④ TO LARGE c_ℓ
3. AVOID FLOW SEPARATION AT ⑤ FOR LARGE α.
4. CONTROL OF PITCHING MOMENT, ⑥.
5. DEVELOP LAMINAR BOUNDARY LAYER FOR HOVER CONDITION, ⑦.

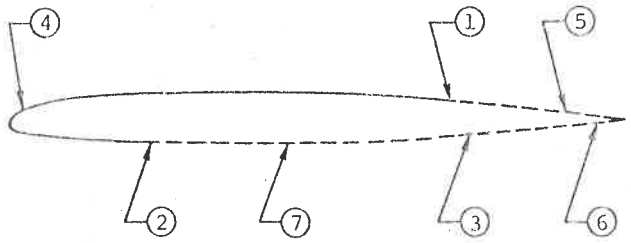

Figure 12. Considerations underlying the modifications to basic shape.

In (1) the freedom to modify the rear parts of the basic airfoil should be used to increase the loading in that region. This, however, is in conflict with the pitching moment requirement and also with (2) and (4), which means that a compromise must be found. This was realized during this study by a trial and error process in which the effect of several modifications on the pressure distribution and the boundary layer flow was calculated by means of a method that combines subsonic, potential flow and boundary layer computations (Reference 18). At the time of this study methods for the computation of transonic flows with shock waves were not yet available at NLR. However, a few check calculations by means of the method of Garabedian and Korn (Reference 19) were made at the end of the investigation.

The final shape shown in Figure 13 resulted from these modifications. Note that the upper surface has been modified aft of 70% x/c and the lower surface aft of 50%.

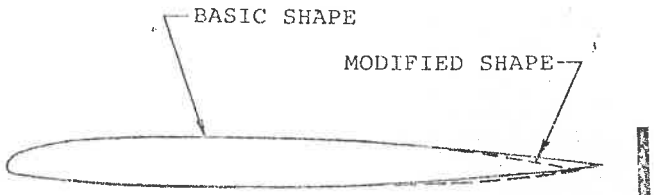

Figure 13. Comparison of basic and modified shapes.

COMPARISON OF NLR AND WORTMANN DESIGNS

Both the NLR 7223-63 and FX-090 airfoils were tested two dimensionally in the United Aircraft Corporation high speed wind tunnel. The Mach number range was from 0.30 to 0.83 with a corresponding Reynolds number range of 2.6 to 5.7 x 10^6. It should be noted that the high Mach number data obtained are questionable because this tunnel has solid walls. Both surface pressure and balance data were taken as well as wake rake data. All force data discussed are based on the integrated surface pressures and the drag data is based on wake rake measurements.

$c_{\ell_{max}}$ and $c_{d_{min}}$ versus Mach number are shown on figures 14 and 15 for the two designs. Figure 16 shows ℓ/d versus c_ℓ for Mach number = 0.6. The degree of performance similarity illustrated in these figures is to be expected since both airfoils were designed to essentially the same criteria.

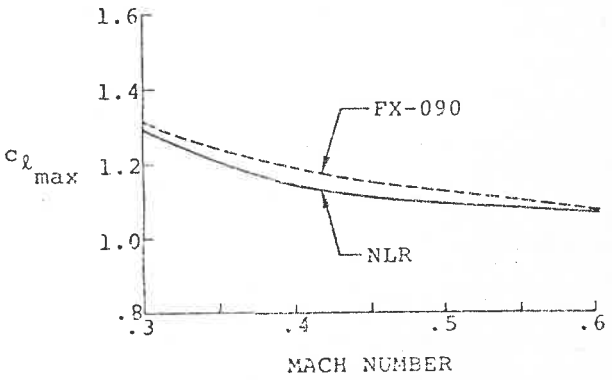

Figure 14. $c_{\ell_{max}}$ vs. Mach number, comparison between the NLR and Wortmann airfoils.

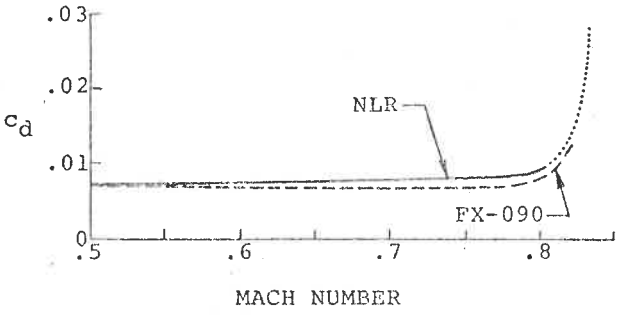

Figure 15. $c_{d_{min}}$ vs. Mach number, comparison between the NLR and Wortmann airfoils.

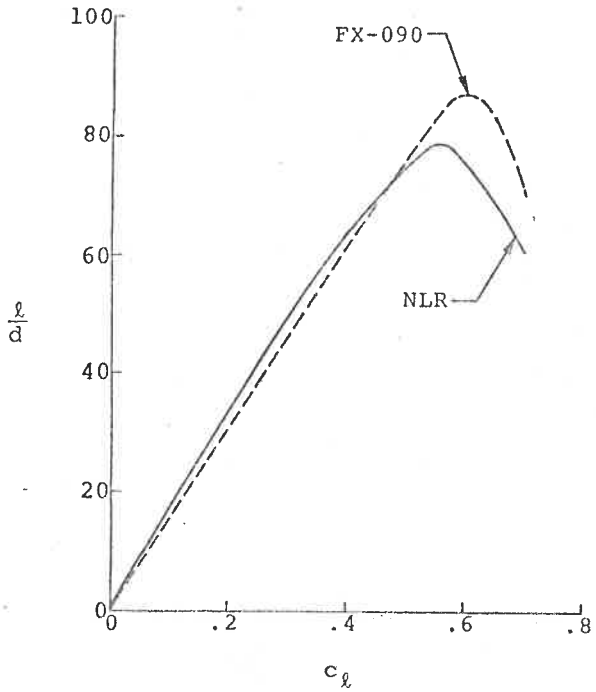

Figure 16. ℓ/d vs. c_ℓ, M = 0.6 comparison between NLR and Wortmann airfoils

A brief evaluation of the NLR 7223-62 test data indicates that some areas of possible improvement may be noted. A comparison of estimated and measured $c_{\ell_{max}}$ at moderate Mach numbers shows that $c_{\ell_{max}}$ at M = 0.5 is somewhat low. It is indeed lower than the predicted value which was obtained by correlating the results of potential flow and boundary layer calculations for the present airfoil and for the FX-098 airfoil with experimental results of the latter.

This lower value of $c_{\ell_{max}}$ is possibly due to a rather early separation of the upper surface boundary layer near the trailing edge. This is reflected by the divergence of the trailing edge pressure as shown in figure 17 for $c_\ell \approx 0.8$. This may explain also why the shock Mach number at c_ℓ is relatively low (about 1.3 as compared to about 1.4 for the FX-098 as shown in Figure 18.

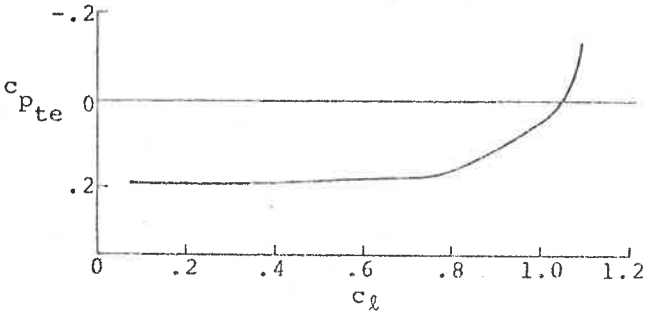

Figure 17. Trailing edge pressure vs. c_ℓ at M_∞ = 0.5 for NLR airfoils.

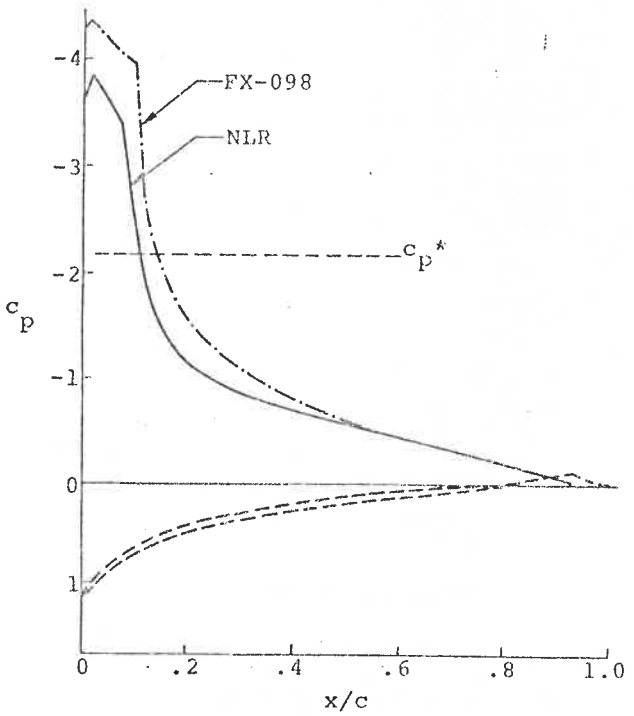

Figure 18. Test data comparison of pressure distribution for the NLR and Wortmann airfoils.

Apparently, the separation of the boundary layer near the trailing edge limits a further growth of the circulation. Some improvement in this respect might be obtained by reshaping the upper surface near the trailing edge in the sense that the pressure gradients are reduced.

At $M_\infty = 0.6$ (hover) the first divergence of the trailing edge pressure is observed to occur at $c_\ell \sim 0.6$ (figure 19). Beyond this value of c_ℓ the drag increases rapidly. As a result the maximum value of ℓ/d is 75-80 at $c_\ell = 0.56$. (Subsonic potential flow and boundary layer calculations, supplemented with results from the Garabedian/Korn program suggested a maximum value of 90 at $c_\ell \sim 0.65$).

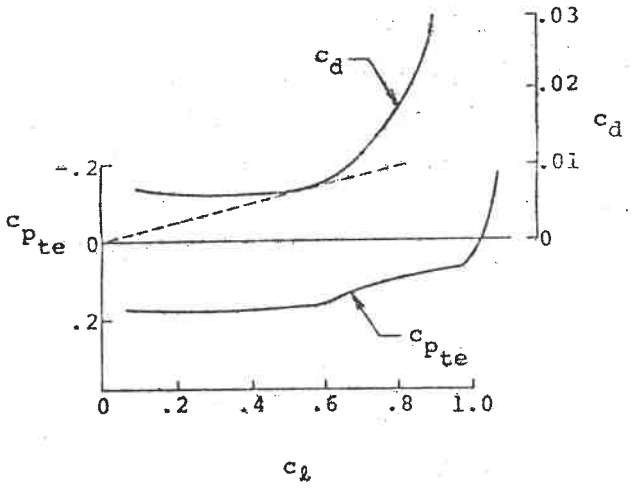

Figure 19. Trailing edge pressure and c_d vs. c_ℓ at M = 0.6 for NLR airfoil.

It is likely that boundary layer separation near the trailing edge is not the only reason for the somewhat early increase of drag at $M_\infty = 0.6$. Pressure distributions for $c_\ell \sim 0.6$ indicate the appearance of a shock on the upper surface (figure 20). The strength of this shock is probably large enough to cause a measurable drag creep.

It may be concluded from this analysis that further improvements are necessary to meet the predicted performance of these sections. It is believed, however, that significant knowledge has been gained in the use of the analytical tools available as well as in the development of an improved airfoil section.

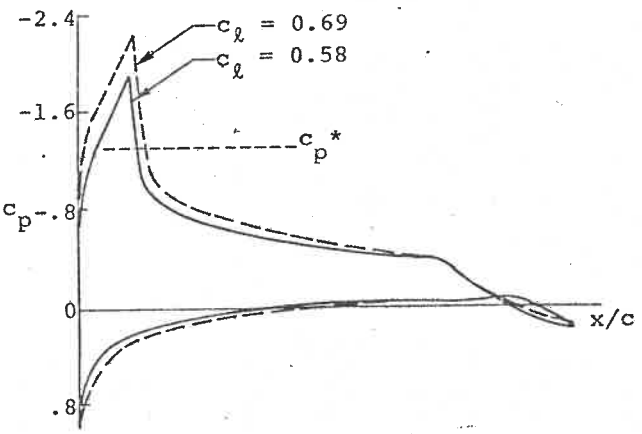

Figure 20. Pressure distribution near hover condition (M = 0.6) for NLR airfoil.

The comparison of wind tunnel test results for the transonic designs with the -098 airfoil does show a useful improvement in drag rise Mach number at low values of lift coefficient. The drag rise Mach number for the transonic designs is about .02 to .025 better than the FX-098. At a given tip speed, this means that forward speed can be increased by 13 to 16 knots or for a given forward speed, tip speed can be increased by 22 to 28 feet per second before drag rise is encountered. This benefit, for the initial effort, is accompanied by an 18 percent decrease in maximum lift coefficient and an 8 to 15 percent decrease in maximum ℓ/d at M = 0.6. This must not be viewed, at this stage, from a pessimistic viewpoint toward the approaches which have been discussed. The level of success achieved by these initial efforts should be an encouragement to perform further analysis and testing upon which basis further improvements can be made in the design techniques.

Application of Initial Designs

The current level of analytical procedures do result, without even any further development, in airfoils which can already be applied to a helicopter design given a specific set of circumstances.

Bell Helicopter, in designing the Model 222 Light Twin Helicopter laid heavy stress on single-engine performance. This emphasis resulted in having sufficient twin-engine power available for hover to enable acceptance of a somewhat reduced hover ℓ/d of a high speed main rotor airfoil to enhance this helicopter's forward speed capability. An 8-percent thick version of a Wortmann-090 type airfoil was developed for the Model 222 main rotor. Flight evaluation of this design is scheduled to begin in early 1976.

A further application of transonic airfoil technology at Bell is found in the Model 645 experimental main rotor blade. This 48-foot diameter, 33-inch chord rotor tapers in thickness from 16 percent at one-quarter radius to 9 percent at the tip. The inboard airfoil is a laminar section transitioning spanwise to the FX-090 airfoil at the tip. Performance of this rotor closely compares to that of a similar rotor equipped with the FX-098 airfoil.

Application of Advanced Designs

Development of the analytical procedures on a solid basis of testing, correlation and refinement will lead to designs which provide increases in drag rise Mach number with minimal compromise in the $c_{\ell_{max}}$ and hover ℓ/d areas. Once this is achieved, helicopter designs can be increased in efficiency by use of higher main rotor tip speeds in conjunction with compressibility-relieving tip shapes. Figure 21 illustrates the calculated performance gains which can be achieved by use of this type of airfoil during a typical high speed mission for a current helicopter. As shown, one may expect an increase in true airspeed for a given rotor tip speed, or other design limitations may be alleviated by an increase in rotor tip speed which is possible with the new section without the expense of additional power.

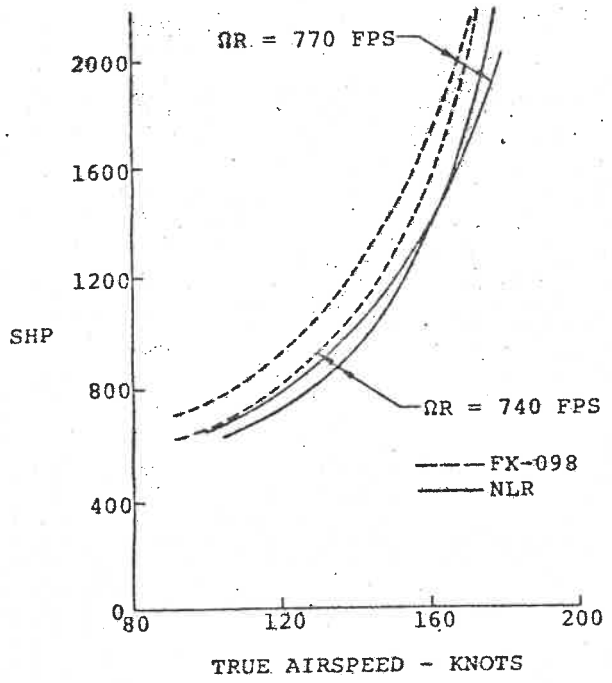

Figure 21. Anticipated high-speed performance gains,

Clark, in Reference 20, clearly pointed out that a design which improves basic performance at the expense of excessive pitching moments is not practical. For this reason, the NASA-NLR-BHC effort included a design with controlled pitching moment (NLR-7223-62) as well as one with no moment limitations imposed (NLR 7223-43). The high-moment design has not been tunnel-tested but the analytical comparisons shown in Table II do not indicate that controlled moment does not handicap the design to any significant degree.

A tunnel test was performed in the low moment design ($c_{m_o} \leq .02$) with a trailing edge reflex to zero out c_{m_o}. Tunnel comparisons show a negligible effect on the airfoil characteristics compared to the unmodified version. Thus a zero-moment design is acceptable with respect to an uncontrolled-moment design.

Table 2. Comparison of Predicted Characteristics as A Function of c_m Control

Condition	Quantity	Uncontrolled c_m	Controlled c_m
$M = 0.6$ $c_\ell = 0.65$	ℓ/d	94	91
$M = 0.5$	$c_{\ell_{max}}$	1.30	1.25
$c_\ell = 0$	M_∞	0.85	0.85

CONCLUSIONS

1. Good high-speed airfoils can be designed today using current methodology.
2. Improvements in the analytical procedures need to be made to improve $c_{\ell_{max}}$ and ℓ/d characteristics of the current design. These improvements will come about only by a series of tests upon which to evaluate and upgrade the analyses.
3. Once the design goals are achieved, the helicopter design will be more flexible due to increasing the range of tip speed available to the designer.

References

1. Wortmann, F.X., "Design of Airfoils for Rotors," CAL/AVLABS 1969 Symposium on Aerodynamics of Rotary Wing and VTOL Aircraft, Buffalo, N. Y.

2. Kemp, Larry D., "An Analytical Study for the Design of Advanced Rotor Airfoils," NASA CR-112297, 1973.

3. Davenport, F. J. & Front, J. V., "Airfoil Sections for Helicopter Rotors - A Reconsideration," 22 Annual Forum of the AHS, Washington, D.C., 1966.

4. Reichert, G., & Wagner, S.N., Some Aspects of the Design of Rotor Airfoil Shapes AGARD Meeting on "The Aerodynamics of Rotary Wings," Marseille 1972, AGARD CP 111

5. Wortmann, F. X., Prepared comment to (3) AGARD CP 111

6. Pearcy, H. H., The Aerodynamic Design of Section Shapes for Swept Wings "Advances in Aeronautical Sciences," Vol. 3, Pergamon Press, London 1962.

7. Truckenbrodt, E., "Die Berechnung der Profilform bei Vorgegebener Geschwindigkeitsverteilung" Ingenieur-Archiv 19 (1951), S.365

8. Riegels, F., "Das Umstromungsproblem," Ingenieur-Archiv 16 (1958) S.373 17 (1949) S.94

9. Labrujere, Th.E., Loeve, W., & Sloof, J. W., "An Approximate Method for the Calculation of the Pressure Distribution on Wingbody Combinations at Subcritical Speeds," Paris 1968 AGARD CP 71

10. Pearcy, H.H., & Osborne, J., "Some Problems and Features of Transonic Aerodynamics," ICAS Congress 1970, Rome.

11. Sinnott, C. S., & Stuart, C.M., "An Analysis of the Supersonic Region in A High Subsonic Flow Past an Airfoil Surface," ARC 21, 715 (1960)

12. Nieuwland, G.Y., Spee, B. M., "Transonic Shockfree Flow, Fact or Fiction?" 1968, AGARD CP 35

13. Wortmann, F.X., "Design of Airfoils with High Lift at Low and Medium Subsonic Mach Numbers," Paper presented at AGARD Specialist's Meeting on the Fluid Dynamics of Aircraft Stalling, Lisbon, 1972.

14. Nieuwland, G.Y., "Transonic Flow Around A Family of Quasi-Elliptical Airfoil Sections," NLR-TR T.172, 1967.

15. Boerstoel, J.W., & Huizing, G.H., "Transonic Shock-Free Airfoil Design by an Analytic Hodograph Method, "AIAA Paper 74-539, 1974.

16. Zwaanevelt, J., & Van Egmond, J. A., "Experimental Results Around the Design Condition of A Quasi-Elliptical Aerofoil Modified for Rear Loading," NLR TR 72078 U, 1972.

17. Stratford, B. S., "An Experimental Flow with Zero Skin Friction Throughout Its Region of Pressure Rise," J. F. M. Vol. 5, January 1959, pps. 17-35.

18. Piers, W. J. & Sloof, J. W., "Calculation of the Displacement Effect in Two-Dimensional, Subsonic, Attached Flow; Examples of Calculations Using Measured Displacement Thicknesses," NLR TR 72116, 1972.

19. Bauer, F., Garabedian, P., and Korn, D., "Supercritical Wing Sections," Berlin: Springer, 1972.

20. Clark, David R., Paglino, V.M., "A Study of the Potential Benefits of Advanced Airfoils for Helicopter Applications," National Symposium on Helicopter Aerodynamic Efficiency, March 1975, Hartford, Conn.